

**A Solvate of the Diacetate Salt of the
Octaethyltetraphenylporphyrin Dication,
 $\text{H}_4\text{OETPP}^{2+} \cdot 2\text{CH}_3\text{COO}^- \cdot 3\text{CH}_3\text{COOH} \cdot$
 CH_2Cl_2**

K. M. BARKIGIA AND J. FAJER

*Department of Applied Science, Brookhaven National
Laboratory, Upton, New York 11973, USA*

M. D. BERBER AND K. M. SMITH

*Department of Chemistry, University of California,
Davis, California 95616, USA*

(Received 3 March 1994; accepted 2 August 1994)

Abstract

The structure of 2,3,7,8,12,13,17,18-octaethyl-5,10,15,-20-tetraphenylporphyrin(2+) diacetate acetic acid dichloromethane solvate, $\text{C}_{60}\text{H}_{64}\text{N}_4^{2+} \cdot 2\text{C}_2\text{H}_3\text{O}_2^- \cdot 3\text{C}_2\text{H}_4\text{O}_2 \cdot \text{CH}_2\text{Cl}_2$, has been determined at 200 K. The molecule is severely non-planar and adopts an S_4 saddle shape. It is the most distorted member of the OETPP series reported to date, with displacements of the β -pyrrole C atoms from the plane of the four N atoms as great as 1.42 Å and acute tilts of the phenyl rings relative to the porphyrin plane. The two acetate counterions act as bidentate ligands which bond to the H atoms on opposite pairs of N atoms. The crystal lattice also contains three acetic acid molecules of solvation

per porphyrin molecule, all of which are involved in hydrogen bonds to the acetate molecules. An 'innocent' molecule of CH_2Cl_2 is also present.

Comment

The diacid salts of porphyrins or their dications ($H_4P^{2+} \cdot 2X^-$) result from the addition of acid to metal-free porphyrin (H_2P) so that all four N atoms of the macrocycle are protonated. Previous studies of 5,10,15,20-tetraphenylporphyrins (TPP) and 5,10,15,20-tetrapyrrolylporphyrins (TPyP), formulated as $H_4TPP^{2+} \cdot Cl^- \cdot FeCl_4^-$ (Stone & Fleischer, 1968), $H_4TPP^{2+} \cdot 2C_2F_3O_2^-$ (Navaza, De Rango & Charpin, 1983; Scheidt & Lee, 1987) and $H_2TPyP \cdot 6HCl \cdot H_2O$ (Stone & Fleischer, 1968), show that the macrocycles are significantly distorted into S_4 saddle shapes, presumably because of steric repulsions between the four central H atoms that cannot be accommodated within the central pocket. An S_4 ruffled distortion was also found in the structure of the 2,3,7,8,12,13,17,18-octaethylporphyrin dication in $H_4OEP^{2+} \cdot 2ClO_4^-$ (Barkigia, Miura, Chang & Fajer, 1988), in sharp contrast to the rigorous planarity observed for the compound $H_4OEP^{2+} \cdot 2[RhCl_2(CO)_2]^-$ (Cetinkaya, Johnson, Lapert, McLaughlin & Muir, 1974). The latter sets of results clearly demonstrate the wide range of conformations that the same porphyrin molecule can adopt, and thus point to the significant plasticity of porphyrin derivatives.

As part of our studies on conformational variations imposed by steric and/or protein constraints, and on the consequences of such distortions on the physical and chemical properties of photosynthetic chromophores, prosthetic groups and synthetic models thereof (Barkigia & Fajer, 1993, and references therein; Fajer *et al.*, 1990), we report here the molecular structure of the diacid salt of OETPP, which crystallizes from mixtures of acetic acid and dichloromethane as $H_4OETPP^{2+} \cdot 2CH_3COO^- \cdot 3CH_3COOH \cdot CH_2Cl_2$. The diacid salt determination extends previous structural characterizations of the OETPP series, which include the free base (Regev *et al.*, 1994) and the Zn (Barkigia *et al.*, 1990), Ni (Barkigia *et al.*, 1993), Co and Cu (Sparks *et al.*, 1993) derivatives, and studies of the effects of the porphyrin pocket occupancy on the conformations of the macrocycles.

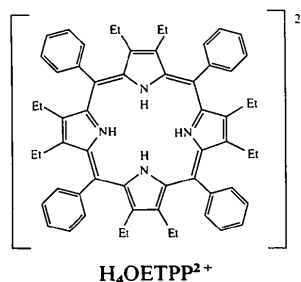


Fig. 1 shows the molecular structure and numbering scheme for the H_4OETPP^{2+} macrocycle. Overall, the porphyrin molecule is quite symmetrical and closely resembles the other OETPP structures. Fig. 2 illustrates the most salient result of this determination, which is the severe S_4 deformation of the macrocycle, and further depicts the hydrogen-bonding interactions of the acetate counterions with the porphyrin. The intrinsically distorted OETPP skeleton, arising from the congestion of adjacent phenyl and ethyl substituents, is further enhanced here. The average displacement of the β -pyrrole C atoms from the plane of the N atoms is 1.37 Å, compared with an average of 1.24 Å in NiOETPP, heretofore the largest in the OETPP series. The distortion is that of a saddle (Fig. 3) with the pyrrole rings displaced alternately up and down by essentially the same distances and the *meso*-C atoms nearly in the plane of the N atoms.

Complementary to the large deviations from planarity is the near coplanarity of the phenyl groups with the porphyrin macrocycle, which has been observed previously in other TPP and TPyP diacids. The dihedral angles of the phenyl rings with the plane of the N

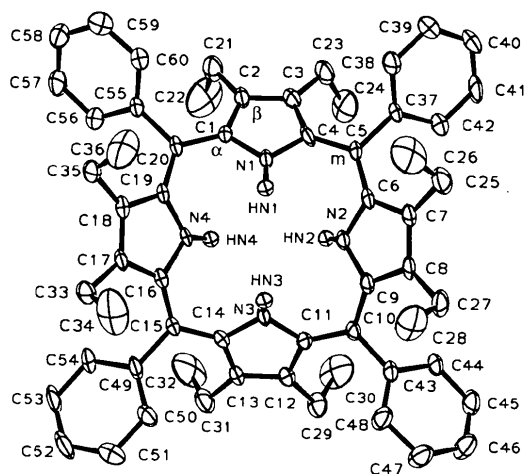


Fig. 1. Molecular structure of H_4OETPP^{2+} at 200 K. Probability ellipsoids are drawn at 50%, except for the H atoms, which are not to scale.

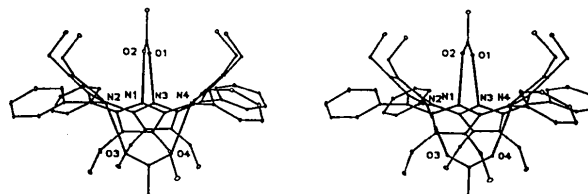


Fig. 2. Stereoscopic edge-on view of the dication and its acetate counterions illustrating the severe S_4 distortion of the macrocycle and the hydrogen bonding of the acetates to the porphyrin.

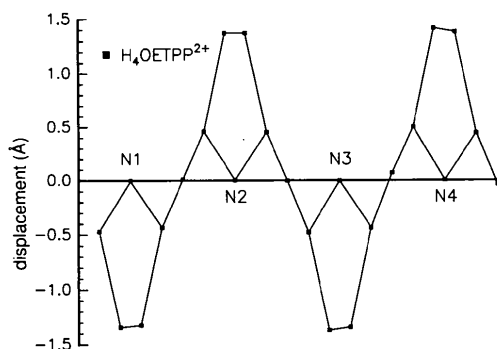


Fig. 3. Linear display of the displacements of the atoms of the macrocycle from the plane of the four N atoms. The ring order is I, II, III, IV from left to right (the horizontal axis is not to scale).

atoms range between $29.2(2)$ and $34.9(2)^\circ$. Those in $\text{H}_4\text{TPP}^{2+} \cdot \text{Cl}^- \cdot \text{FeCl}_4^-$ are the most acute, 21.1° , while they range from 33.0 to 35.6° in $\text{H}_4\text{TPyP}^{2+}$ and from 30.6 to 35.7° in $\text{H}_4\text{TPP}^{2+} \cdot 2\text{C}_2\text{F}_3\text{O}_2^- \cdot \text{UO}_2^{2+} \cdot 2\text{C}_2\text{F}_3\text{O}_2^-$.

A comparison of average bond distances in the six OETPP structures is presented in the deposited material. Particularly noteworthy in all the structures are the 'normal' distances between the *meso*-C atoms and the phenyl rings, contrary to the suggestion of Hoard (1975) that smaller dihedral angles would result in increased conjugation between the porphyrin and phenyl rings. Indeed, in the present structure, the shortest $\text{C}_m\text{—C}_\varphi$ bond of $1.464(7)$ Å occurs at $\text{C}10\text{—C}43$, but does not correspond to the most acute phenyl dihedral angle of $29.2(2)^\circ$ at $\text{C}15$. The $\text{C}_m\text{—C}_\varphi$ distances to the other rings are $1.488(7)$, $1.485(7)$ and $1.481(7)$ Å.

The bond angles in $\text{H}_4\text{OETPP}^{2+}$ vary dramatically. Among those affected are the $\text{C}_\alpha\text{—N—C}_\alpha$ angles which average $109.7(5)^\circ$. They are broadened several degrees with respect to those in the MOETPP structures and are intermediate between the values in the protonated and unprotonated rings of H_2OETPP [$111.0(12)$ and $106.1(11)^\circ$, respectively]. Also discernible is the average contraction of the $\text{N—C}_\alpha\text{—C}_\beta$ angles to $107.5(5)^\circ$, which is common to protonated pyrrole rings (Hoard, 1975; Barkigia *et al.*, 1992) and in agreement with the average of $107.1(12)^\circ$ found in the protonated rings of H_2OETPP . While the $\text{C}_\beta\text{—C}_\alpha\text{—C}_m$ angles are constant across the remainder of the series, ranging from $127.9(5)$ to $128.8(13)^\circ$, they are opened to $130.7(5)^\circ$ in the diacid.

As in all the other porphyrin dications studied to date, the counterions are hydrogen bonded to the macrocycle. The O atoms O2 and O1 of one acetate flank opposite pairs of N atoms at distances of $2.707(6)$ and $2.741(6)$ Å, respectively, while atoms O3 and O4 of the second acetate bridge atoms N2 and N4 at distances of $2.747(6)$ and $2.753(6)$ Å, respectively. They are clearly acetate rather than acetic acid molecules, as evidenced by the equivalent C—O bonds in both

species. In turn, the acetates are hydrogen bonded to the three acetic acid molecules in an asymmetrical fashion, as only three of the four acetate O atoms participate in hydrogen bonds. These are strong hydrogen bonds with short O...O contact distances of $2.544(7)$, $2.586(6)$ and $2.548(6)$ Å. From the disparate C—O distances, these secondary hydrogen-bonded species are clearly acetic acid molecules.

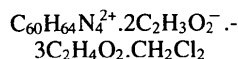
Since the diacid molecules are capped on both sides by acetates and insulated by acetic acid molecules, the shortest center-to-center distance is 11.46 Å, and the mean plane separation between these inversion-related molecules is 11.02 Å.

The additional molecule of solvation, CH_2Cl_2 , found in the crystal appears to be 'innocent', as it is well separated from the remainder of the atoms. Its closest contact involves atom C11 and an inversion-related C11 atom at a distance of 7.07 Å.

Traditionally, it has been assumed that the large optical red shifts observed for *meso*-tetraarylporphyrin dications are due to increased conjugation of the aryl rings with the porphyrin because of their increased coplanarities (Stone & Fleischer, 1968; Hoard, 1975). However, the entire OETPP series and several other saddle-shaped porphyrins with varying degrees of porphyrin-aryl ring dihedral angles also exhibit significant bathochromic optical shifts (Barkigia, Chantranupong, Smith & Fajer, 1988; Renner, Cheng, Chang & Fajer, 1990; Bhyrappa, Krishnan & Nethaji, 1993; Barkigia *et al.*, 1993). It is likely, therefore, that the saddle distortions of the diacid salts contribute at least in part to the observed red shifts. Molecular-orbital calculations do indeed predict such shifts because of the destabilization of the porphyrin π system caused by the conformational distortions (Barkigia, Chantranupong, Smith & Fajer, 1988; Barkigia *et al.*, 1993; Sparks *et al.*, 1993).

Experimental

Crystal data



$M_r = 1224.4$

Triclinic

$P\bar{1}$

$a = 13.684(5)$ Å

$b = 20.294(5)$ Å

$c = 13.090(4)$ Å

$\alpha = 98.64(2)^\circ$

$\beta = 107.98(3)^\circ$

$\gamma = 91.06(2)^\circ$

$V = 3410.2$ Å³

$Z = 2$

$D_x = 1.192$ Mg m⁻³

Cu $K\alpha$ radiation

$\lambda = 1.5418$ Å

Cell parameters from 25 reflections

$\theta = 17\text{--}25^\circ$

$\mu = 1.318$ mm⁻¹

$T = 200$ K

Irregular block

$0.66 \times 0.26 \times 0.20$ mm

Green

Crystal source: from acetic acid/ CH_2Cl_2 solution

Data collection

Enraf-Nonius CAD-4 diffractometer

6743 observed reflections
[$F_o > 3\sigma(F_o)$]

ω -2 θ scans
 Absorption correction:
 analytical
 $T_{\min} = 0.613$, $T_{\max} = 0.786$
 13 038 measured reflections
 10 077 independent reflections

$R_{\text{int}} = 0.022$
 $\theta_{\text{max}} = 60^\circ$
 $h = -15 \rightarrow 15$
 $k = -22 \rightarrow 22$
 $l = -14 \rightarrow 14$
 3 standard reflections
 frequency: 60 min
 intensity decay: within counting statistics

Refinement

Refinement on F $R = 0.095$ $wR = 0.119$ $S = 3.17$

6743 reflections

784 parameters

H-atom parameters not

refined

 $w = 4F_o^2 / [\sigma^2(F_o^2) + (0.05F^2)^2]$ $(\Delta/\sigma)_{\text{max}} = 0.015$ $\Delta\rho_{\text{max}} = 0.90 \text{ e } \text{\AA}^{-3}$ $\Delta\rho_{\text{min}} = -0.96 \text{ e } \text{\AA}^{-3}$

C45	0.2611 (5)	0.8112 (3)	-0.1793 (5)	0.041 (2)
C46	0.2919 (5)	0.8606 (3)	-0.2254 (5)	0.046 (2)
C47	0.3933 (5)	0.8853 (3)	-0.1904 (6)	0.049 (2)
C48	0.4655 (5)	0.8610 (3)	-0.1049 (5)	0.041 (2)
C49	0.9526 (4)	0.7844 (3)	0.1085 (5)	0.032 (2)
C50	0.9368 (5)	0.8317 (3)	0.0385 (5)	0.040 (2)
C51	1.0125 (6)	0.8471 (4)	-0.0038 (6)	0.054 (3)
C52	1.1040 (5)	0.8167 (4)	0.0216 (6)	0.051 (3)
C53	1.1192 (4)	0.7682 (4)	0.0869 (6)	0.045 (2)
C54	1.0448 (4)	0.7517 (3)	0.1313 (5)	0.039 (2)
C55	0.9320 (4)	0.6848 (3)	0.5871 (5)	0.030 (2)
C56	1.0139 (5)	0.6478 (3)	0.5702 (5)	0.041 (2)
C57	1.0890 (5)	0.6310 (3)	0.6597 (6)	0.048 (3)
C58	1.0861 (5)	0.6501 (4)	0.7640 (6)	0.049 (3)
C59	1.0058 (5)	0.6844 (4)	0.7796 (5)	0.052 (3)
C60	0.9284 (5)	0.7022 (3)	0.6921 (5)	0.039 (2)
O1	0.7125 (3)	0.8850 (2)	0.2801 (4)	0.046 (1)
O2	0.7068 (4)	0.8565 (2)	0.4351 (4)	0.049 (2)
C61	0.7182 (5)	0.8985 (3)	0.3789 (6)	0.035 (2)
C62	0.7404 (7)	0.9703 (4)	0.4313 (6)	0.064 (3)
O3	0.5621 (3)	0.6310 (2)	0.1588 (4)	0.046 (1)
O4	0.7304 (3)	0.6198 (2)	0.2085 (4)	0.045 (1)
C63	0.6383 (5)	0.5958 (3)	0.1708 (5)	0.040 (2)
C64	0.6181 (5)	0.5222 (3)	0.1391 (7)	0.065 (3)
O5	0.7827 (4)	0.9768 (2)	0.2037 (4)	0.064 (2)
O6	0.7126 (4)	0.9202 (3)	0.0371 (4)	0.075 (2)
C65	0.7679 (6)	0.9648 (4)	0.0979 (7)	0.048 (3)
C66	0.8349 (6)	1.0133 (4)	0.0662 (6)	0.062 (3)
O7	0.3785 (4)	0.5739 (2)	0.1013 (4)	0.062 (2)
O8	0.3117 (4)	0.6646 (3)	0.0554 (6)	0.107 (3)
C67	0.3017 (5)	0.6098 (4)	0.0657 (6)	0.045 (3)
C68	0.1990 (6)	0.5735 (4)	0.0459 (7)	0.074 (3)
O9	0.8719 (4)	0.5390 (2)	0.2159 (5)	0.081 (2)
O10	0.9839 (4)	0.6233 (3)	0.2678 (6)	0.105 (3)
C69	0.9655 (5)	0.5656 (4)	0.2456 (6)	0.052 (3)
C70	1.0458 (6)	0.5162 (5)	0.2482 (10)	0.106 (5)
C15	0.2965 (8)	0.1081 (6)	0.3353 (11)	0.138 (6)
C11	0.2027 (4)	0.0452 (2)	0.2477 (3)	0.187 (2)
C12	0.2931 (3)	0.1753 (3)	0.2645 (5)	0.239 (3)

Table 1. Fractional atomic coordinates and equivalent isotropic displacement parameters (\AA^2)

$$U_{\text{eq}} = (1/3) \sum_i \sum_j U_{ij} a_i^* a_j^* \mathbf{a}_i \cdot \mathbf{a}_j$$

	x	y	z	U_{eq}
N1	0.6719 (3)	0.7228 (2)	0.4160 (4)	0.029 (1)
N2	0.5205 (3)	0.7605 (2)	0.2182 (4)	0.024 (1)
N3	0.6874 (3)	0.7748 (2)	0.1227 (4)	0.024 (1)
N4	0.8398 (3)	0.7384 (2)	0.3169 (4)	0.026 (1)
C1	0.7482 (4)	0.6863 (3)	0.4718 (5)	0.028 (2)
C2	0.7006 (4)	0.6336 (3)	0.5047 (5)	0.031 (2)
C3	0.5956 (4)	0.6418 (3)	0.4727 (5)	0.034 (2)
C4	0.5787 (4)	0.6998 (3)	0.4200 (4)	0.030 (2)
C5	0.4887 (4)	0.7327 (3)	0.3789 (4)	0.025 (2)
C6	0.4745 (4)	0.7719 (3)	0.2970 (5)	0.027 (2)
C7	0.4096 (4)	0.8266 (3)	0.2744 (5)	0.027 (2)
C8	0.4138 (4)	0.8436 (3)	0.1783 (5)	0.027 (2)
C9	0.4816 (4)	0.7995 (3)	0.1396 (5)	0.025 (2)
C10	0.5057 (4)	0.7918 (3)	0.0420 (5)	0.025 (2)
C11	0.5991 (4)	0.7660 (3)	0.0338 (4)	0.025 (2)
C12	0.6247 (4)	0.7335 (3)	-0.0584 (5)	0.027 (2)
C13	0.7299 (4)	0.7275 (3)	-0.0245 (5)	0.028 (2)
C14	0.7697 (4)	0.7562 (3)	0.0882 (5)	0.026 (2)
C15	0.8730 (4)	0.7698 (3)	0.1590 (5)	0.025 (2)
C16	0.8983 (4)	0.7730 (3)	0.2708 (5)	0.025 (2)
C17	0.9851 (4)	0.8058 (3)	0.3591 (5)	0.027 (2)
C18	0.9788 (4)	0.7871 (3)	0.4542 (5)	0.027 (2)
C19	0.8889 (4)	0.7424 (3)	0.4260 (5)	0.025 (2)
C20	0.8540 (4)	0.7048 (3)	0.4923 (5)	0.029 (2)
C21	0.7498 (5)	0.5749 (3)	0.5511 (6)	0.045 (2)
C22	0.7567 (9)	0.5203 (5)	0.4644 (9)	0.109 (5)
C23	0.5117 (5)	0.5927 (3)	0.4749 (6)	0.047 (2)
C24	0.4535 (6)	0.5560 (4)	0.3654 (7)	0.072 (3)
C25	0.3606 (5)	0.8652 (3)	0.3515 (6)	0.044 (2)
C26	0.4435 (7)	0.9055 (4)	0.4521 (7)	0.082 (4)
C27	0.3725 (4)	0.9041 (3)	0.1326 (5)	0.039 (2)
C28	0.4515 (6)	0.9627 (4)	0.1608 (7)	0.073 (3)
C29	0.5498 (5)	0.7043 (3)	-0.1680 (5)	0.039 (2)
C30	0.4892 (7)	0.6430 (4)	-0.1612 (7)	0.085 (4)
C31	0.7892 (5)	0.6884 (3)	-0.0895 (5)	0.043 (2)
C32	0.8098 (8)	0.6222 (4)	-0.0642 (8)	0.094 (5)
C33	1.0620 (4)	0.8585 (3)	0.3540 (5)	0.037 (2)
C34	1.0196 (7)	0.9251 (4)	0.3467 (9)	0.091 (4)
C35	1.0433 (4)	0.8171 (3)	0.5665 (5)	0.040 (2)
C36	0.9898 (7)	0.8692 (4)	0.6217 (6)	0.079 (3)
C37	0.4039 (4)	0.7253 (3)	0.4261 (5)	0.029 (2)
C38	0.4198 (5)	0.7396 (4)	0.5380 (5)	0.049 (2)
C39	0.3416 (5)	0.7322 (4)	0.5810 (6)	0.058 (3)
C40	0.2429 (5)	0.7111 (4)	0.5109 (6)	0.056 (3)
C41	0.2246 (4)	0.6964 (4)	0.4012 (6)	0.049 (3)
C42	0.3022 (4)	0.7041 (3)	0.3569 (5)	0.039 (2)
C43	0.4331 (4)	0.8129 (3)	-0.0535 (5)	0.030 (2)
C44	0.3300 (4)	0.7877 (3)	-0.0924 (5)	0.031 (2)

Table 2. Selected geometric parameters (\AA , $^\circ$)

N1—C1	1.375 (6)	N1—C4	1.368 (7)
N2—C6	1.359 (7)	N2—C9	1.375 (7)
N3—C11	1.381 (7)	N3—C14	1.377 (7)
N4—C16	1.379 (7)	N4—C19	1.368 (7)
C1—C2	1.428 (7)	C3—C4	1.439 (8)
C6—C7	1.443 (7)	C8—C9	1.451 (7)
C11—C12	1.429 (8)	C13—C14	1.430 (8)
C16—C17	1.443 (7)	C18—C19	1.432 (7)
C2—C3	1.388 (8)	C7—C8	1.370 (8)
C12—C13	1.384 (7)	C17—C18	1.381 (8)
C4—C5	1.407 (7)	C5—C6	1.398 (7)
C9—C10	1.403 (8)	C10—C11	1.419 (7)
C14—C15	1.425 (7)	C15—C16	1.386 (7)
C19—C20	1.416 (7)	C20—C1	1.421 (7)
C5—C37	1.488 (7)	C10—C43	1.464 (7)
C15—C49	1.485 (7)	C20—C55	1.481 (7)
N1—O2	2.707 (6)	N2—O3	2.747 (6)
N3—O1	2.741 (6)	N4—O4	2.753 (6)
O1—O5	2.544 (7)	O3—O7	2.586 (6)
O4—O9	2.548 (6)		
N1—C1—C2	108.2 (5)	N1—C4—C3	107.5 (5)
N2—C6—C7	107.5 (5)	N2—C9—C8	106.6 (5)
N3—C11—C12	108.2 (5)	N3—C14—C13	107.6 (5)
N4—C16—C17	106.6 (5)	N4—C19—C18	107.7 (5)
C1—N1—C4	109.5 (4)	C6—N2—C9	110.3 (4)
C11—N3—C14	108.8 (5)	C16—N4—C19	110.2 (4)
C1—C2—C3	107.0 (5)	C2—C3—C4	107.7 (5)
C6—C7—C8	107.5 (5)	C7—C8—C9	107.6 (5)
C11—C12—C13	107.0 (5)	C12—C13—C14	108.0 (5)
C16—C17—C18	107.9 (5)	C17—C18—C19	107.4 (5)
C2—C1—C20	130.7 (5)	C3—C4—C5	131.2 (5)
C5—C6—C7	129.8 (5)	C8—C9—C10	131.1 (5)
C10—C11—C12	130.8 (5)	C13—C14—C15	131.0 (5)
C15—C16—C17	131.4 (5)	C18—C19—C20	129.3 (5)
C4—C5—C6	123.9 (5)	C9—C10—C11	122.2 (5)

C14—C15—C16	122.2 (5)	C19—C20—C1	122.7 (5)
N1—C1—C20	121.4 (5)	N1—C4—C5	121.4 (5)
N2—C6—C5	122.5 (5)	N2—C9—C10	122.3 (5)
N3—C11—C10	120.9 (5)	N3—C14—C15	121.2 (5)
N4—C16—C15	121.9 (5)	N4—C19—C20	122.9 (5)

The central H atoms, HN1, HN2, HN3 and HN4, were located from a difference Fourier map using the data with $\sin\theta/\lambda < 0.5 \text{ \AA}^{-1}$. The H atoms of the CH_2Cl_2 molecule of solvation and the acid protons of the three acetic acid molecules were not included in the model. Scattering factors for the non-H atoms were taken from Cromer & Mann (1968) and Cromer & Liberman (1970), and those for the H atoms from Stewart, Davidson & Simpson (1965). Anomalous terms for the Cl atoms were taken from Cromer (1974). The high final *R* value is attributed to the high thermal motion of some of the atoms of the solvent molecules and the marginal quality of the crystal, which was the only one in the sample.

Data collection: *CAD-4 Operations Manual* (Enraf–Nonius, 1977). Cell refinement: *CAD-4 Operations Manual*. Data reduction: *CRYSNET* (Berman, Bernstein, Bernstein, Koetzle & Williams, 1976). Structure solution: *SHELXS86* (Sheldrick, 1985). Molecular graphics: *ORTEPII* (Johnson, 1976) and *GENPLOT* (Computer Graphics Service, 1989).

This work was supported by the Division of Chemical Sciences, US Department of Energy, under contract DE-AC02-76CH00016 at BNL, and by National Science Foundation grant CHE-93-05577 at the University of California.

Lists of structure factors, anisotropic displacement parameters, H-atom coordinates and comparison distances and angles in a series of OETPP's, and also a packing diagram and a view of the hydrogen bonding of the acetic acid molecules to the acetates have been deposited with the IUCr (Reference: BK1046). Copies may be obtained through The Managing Editor, International Union of Crystallography, 5 Abbey Square, Chester CH1 2HU, England.

References

- Barkigia, K. M., Berber, M. D., Fajer, J., Medforth, C. J., Renner, M. W. & Smith, K. M. (1990). *J. Am. Chem. Soc.* **113**, 8851–8857.
- Barkigia, K. M., Chantranupong, L., Smith, K. M. & Fajer, J. (1988). *J. Am. Chem. Soc.* **110**, 7566–7567.
- Barkigia, K. M. & Fajer, J. (1993). *The Photosynthetic Reaction Center*, Vol. 2, edited by H. Deisenhofer & J. R. Norris, pp. 513–539. San Diego: Academic Press.
- Barkigia, K. M., Miura, M., Chang, C. K. & Fajer, J. (1988). *Am. Chem. Soc. Div. Inorg. Chem.* Abstract 0305.
- Barkigia, K. M., Renner, M. W., Furenlid, L. R., Medforth, C. J., Smith, K. M. & Fajer, J. (1993). *J. Am. Chem. Soc.* **115**, 3627–3637.
- Barkigia, K. M., Thompson, M. A., Fajer, J., Pandey, R. K., Smith, K. M. & Vicente, M. G. H. (1992). *New J. Chem.* **16**, 599–607.
- Berman, H. M., Bernstein, F. C., Bernstein, H. J., Koetzle, T. F. & Williams, G. J. B. (1976). *CRYSNET*. Informal Report BNL21714. Brookhaven National Laboratory, Upton, USA.
- Bhyrappa, P., Krishnan, V. & Nethaji, M. (1993). *J. Chem. Soc. Dalton Trans.* pp. 1901–1906.
- Cetinkaya, E., Johnson, A. W., Lappert, M. F., McLaughlin, G. M. & Muir, K. W. (1974). *J. Chem. Soc. Dalton Trans.* pp. 1236–1243.
- Computer Graphics Service (1989). *GENPLOT*. Computer Graphics Service, Ithaca, New York, USA.

- Cromer, D. T. (1974). *International Tables for X-ray Crystallography*, Vol. IV, pp. 149–151. Birmingham: Kynoch Press. (Present distributor Kluwer Academic Publishers, Dordrecht.)
- Cromer, D. T. & Liberman, D. (1970). *J. Chem. Phys.* **53**, 1891–1898.
- Cromer, D. T. & Mann, J. B. (1968). *Acta Cryst.* **A24**, 321–324.
- Enraf–Nonius (1977). *CAD-4 Operations Manual*. Enraf–Nonius, Delft, The Netherlands.
- Fajer, J., Barkigia, K. M., Gudowska-Nowak, E., Zhong, E., Smith, K. M. & Newton, M. D. (1990). *Reaction Centers of Photosynthetic Bacteria*, edited by M. Michel-Beyerle, pp. 367–376. Berlin: Springer-Verlag.
- Hoard, J. L. (1975). *Porphyryns and Metalloporphyryns*, edited by K. M. Smith, pp. 317–380. Amsterdam: Elsevier.
- Johnson, C. K. (1976). *ORTEPII*. Report ORNL-5138. Oak Ridge National Laboratory, Tennessee, USA.
- Navaza, A., De Rango, C. & Charpin, P. (1983). *Acta Cryst.* **C39**, 1625–1628.
- Regev, A., Galili, T., Medforth, C. J., Smith, K. M., Barkigia, K. M., Fajer, J. & Levanon, H. (1994). *J. Phys. Chem.* **98**, 2520–2526.
- Renner, M. W., Cheng, R. J., Chang, C. K. & Fajer, J. (1990). *J. Phys. Chem.* **94**, 8508–8511.
- Scheidt, W. R. & Lee, Y. J. (1987). *Struct. Bonding (Berlin)*, **64**, 1–70.
- Sheldrick, G. M. (1985). *Crystallographic Computing 3*, edited by G. M. Sheldrick, C. Krüger & R. Goddard, pp. 175–189. Oxford Univ. Press.
- Sparks, L. D., Medforth, C. J., Park, M.-S., Chamberlain, J. R., Ondrias, M. R., Senge, M. O., Smith, K. M. & Shelnutz, J. A. (1993). *J. Am. Chem. Soc.* **115**, 581–592.
- Stewart, R. F., Davidson, E. R. & Simpson, W. T. (1965). *J. Chem. Phys.* **42**, 3175–3187.
- Stone, A. & Fleischer, E. B. (1968). *J. Am. Chem. Soc.* **90**, 2735–2748.